Available online www.jocpr.com

Journal of Chemical and Pharmaceutical Research, 2016, 8(8):71-81

Research Article

ISSN : 0975-7384
CODEN(USA) : JCPRC5

Synthesis, characterization and humidity sensor application of Poly(methylorange) based triblock copolymer

A. Murugesan*, K. Jeevanandham, S. Palanikumar and R. Anbarasan

Department of Polymer Technology, Kamaraj College of Engineering and Technology, Virudhunagar – 626 001, Tamilnadu, India

ABSTRACT

Synthesis, characterization and its humidity sensor application of Poly(methyl orange) (PMO) was done under inert atmosphere. In order to increase the molecular weight and processability it was block copolymerized with ε-caprolactone (CL) and tetrahydrofuran (THF) separately. The conductivity value of PMO was found to be decreased after the chemical conjugation with poly(ε-caprolctone) (PCL) and poly(tetrahydrofuran) (PTHF) blocks. Thus obtained triblock copolymer was subjected to humidity sensor application and the results are critically compared. The triblocks were further characterized by fourier transform infrared (FTIR) spectroscopy, UV-visible spectroscopy, Fluorescence spectroscopy, differential scanning calorimetry (DSC), thermogravimetric analysis (TGA), gel permeation chromatography (GPC), field emission scanning electron microscopy (FESEM) and cyclic voltammetry (CV).

Keywords: Synthesis, Ring opening polymerization, Conductivity, Humidity sensor study

INTRODUCTION

A tremendous research work is carried out in the conducting polymer field and the discovery of a new member in the conducting polymer (organic electronics) family received the Nobel prize in Chemistry, in the year 2000. This urged us to synthesize a new type of conducting polymer towards the sensor application. This is the motivation behind the present investigation. Organic electronic materials are called synthetic metals due to their high electrical conductivity value. There is a considerable interest towards the synthesis and application of electrically conducting poly(dyes), apart from the various conducting polymers to bio-medical sensor due to its ease of synthesis, good redox potential with excellent environmental stability. For example, poly(methyleneblue) modified electrode was synthesized and its electrochelation and spectroelectrochelation studies were reported by Tan et al. [1]. In 2007, poly(eriochrome black T) was synthesized and its application to dopamine, ascorbic acid determination was studied [2]. Poly(malachite green) was synthesized for the determination of dopamine [3]. Electrochelation preparation of poly(bromothymol blue) film and its analytical application were studied by Xu and co-workers [4]. Poly(neutral red) was prepared and its Raman spectroelectrochemical study was reported in the literature [5]. Other authors also studied the synthesis and application of various poly(dyes) [6-12]. Through thorough literature survey, we could not find any report based on the synthesis and sensor application of poly(methyl orange). Methyl Orange (MO) is an azo type dye [13-15]. Even then, its poor bio-compatibility and bio-degradability restricted its application to some extent. This can be solved by the block copolymerization with CL.

Polycaprolactone (PCL) is one of the bio-compatible and bio-degradable polymers with excellent flexibility. PCL can be synthesized by ring opening polymerization (ROP) of CL in the presence of Stannous octoate (SO) as a catalyst. Hydrogen phosphonate initiated ROP of CL was reported in the literature [16]. Zhong and co-workers [17] made a comparative study on the ROP of CL and L-lactide in the presence of calcium methoxide as an initiator. A hetero nucleo-base functionalized PCL was reported in the literature [18]. Recently, Anbarasan and research team

[19-21] studied the various dye initiated ROP of CL. Other research team also studied the ROP of CL using different chemical initiators [22-25]. A very few reports are available on the poly(dye) initiated ROP of CL. After the diblock copolymerization there is a chance for the decrease of electrical conductivity and solubility of poly(dye). These problems can be outwitted by the ROP of THF in the presence of diblock copolymer.

Poly(tetrahydrofuran) (PTHF) is a tetrahydrofuronium end capped polyether with hydrophilic character. Cationic initiated ROP of THF lead to the formation of PTHF [26]. Other initiators were also used for the ROP of THF [27-30]. Through thorough literature survey, we could not find any report based on the poly(dye) based diblock copolymer initiated ROP of THF. The novelty of the present investigation is a dye based polymer which acts as a macro initiator. To the best of our knowledge, this is the first report.

EXPERIMENTAL SECTION

Materials

Methyl orange (M.O) and methanol were purchased from CDH, India. Caprolactone (CL) was purchased from Sigma Aldrich, India. Stannous octoate (SO) was purchased from Merck, India. Diethyl ether, chloroform and tetrahydrofuran (THF) were purchased from S.D fine chemicals, India and are used as such.

In the present investigation, the targeted product was synthesized in three steps as mentioned below.

Methods

Synthesis of Poly(methyl orange) (PMO)

4g M.O dye was dissolved in 100 mL ethanol and doped with 250 mL 1M HCl under vigorous stirring. 2g $FeCl_3$ in 100 mL double distilled (DD) water was slowly added under mild stirring condition with N_2 purging at 0-5^oC. The colour of the reaction medium became dark brown. This confirmed the dimerization reaction [31-32]. The stirring was continued for another 6 hours. At the end of the reaction the medium became yellowish brown and dried at 110^oC for 8 hours. The precipitate was weighed and stored in a zip lock cover. The yield was noted as 80%. During the chemical polymerization of M.O, the Fe^{3+} was reduced to Fe^0 (i.e) iron metal nano particle.

Synthesis of Poly(caprolactone)-b-Poly(methyl orange)-Poly(caprolactone) triblock copolymer

0.2g PMO was taken in a 25 mL round bottomed (RB) flask equipped with N_2 inlet and outlet. Here the PMO is acting as a macro initiator. 2g CL was accurately weighed and discharged into the RB flask. 0.001g S.O catalyst was added and the [M/C] was maintained at 1000. The temperature of the reaction mixtures were raised to 160^0C with mild stirring condition. The reaction was allowed to continue for the next 2 hours. During the course of the reaction, the medium became highly viscous because of the bulk polymerization of CL. After 2 hours of ROP, the RB flask was taken from the oil bath and cooled. The contents were dissolved in $CHCl_3$ (25 mL) and re-precipitated by adding 200 mL ether taken in a 500 mL beaker [19,20]. The beaker was kept under fume hood overnight to dry the sample. Thus the purified sample (triblockcopolymer) was weighed and stored in a zipper lock cover. The yield was noted as 99%.

Synthesis of PTHF end functionalized triblock copolymer

The polymer obtained in the second stage was dissolved in 25mL of THF (also acting as a co-monomer). The ROP of THF was initiated by adding 0.001g PAH. The ROP of THF was carried out at 45^oC under N_2 atmosphere for 8 hours [29]. At the end of the reaction, the unreacted THF was allowed to evaporate. 20 mL of DD water was added to the contents in the flask and was again subjected to heating at 110^oC. Due to the process all the unreacted THF was removed. Thus purified polymer was weighed and stored in a zipper lock cover. The yield was noted as 65%.

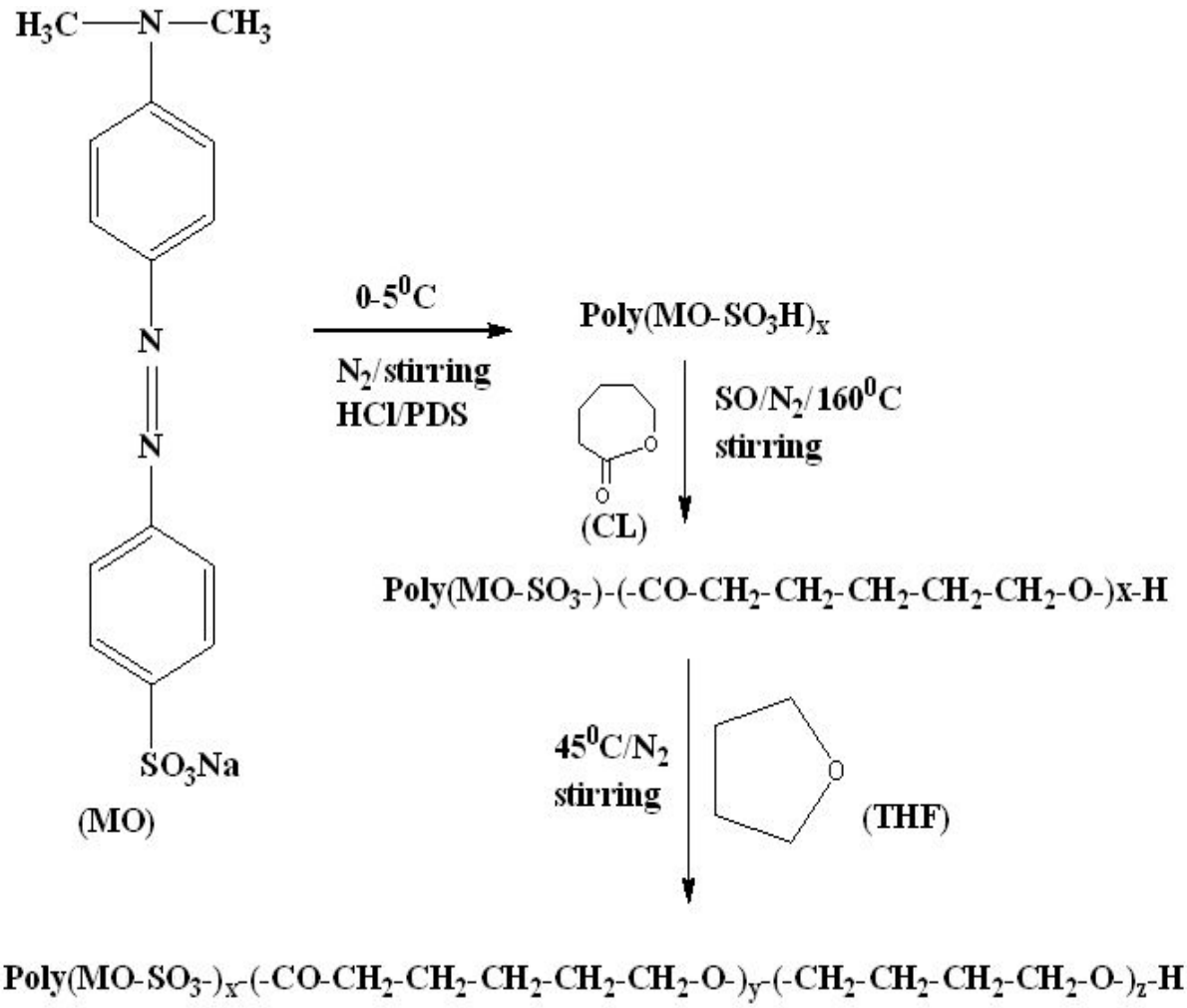

Scheme-1. Synthesis of PMO-PCL-PTHF triblock copolymer

Characterization

The above synthesized samples were characterized by the following techniques. A Jasco V-570 instrument was used for UV–visible spectrum measurement in THF solvent. Fluorescence measurement was carried out with the help of an instrument Elico SL 172, India. FTIR spectra for the samples were recorded with the help of a Shimadzu 8400 S, Japan instrument by the KBr pelletization method from 400 to 4000 cm^{-1}. Differential scanning calorimetry (DSC) and Thermogravimetric analysis (TGA) were measured by using Universal V4.4A TA Instruments under nitrogen atmosphere at the heating rate of 10 K min^{-1} from room temperature to 373 K. The second heating scan of the sample was considered to delete the previous thermal history of the sample. The surface morphology and particle sizes of the grafted samples were determined by FE-SEM, Hitachi S4800 Japan instrument. Four probe method was used to study the conductivity characteristics of synthesized samples. Molecular weight determination of triblock copolymer samples was carried out by using gel permeation chromatography, Perkin Elmer Series 200.

RESULTS AND DISCUSSION

FTIR spectroscopy

The structure of polymer is confirmed through the identification of functional groups. Fig. **1**a indicates the FTIR spectrum of PMO. The aromatic benzenoid stretching and quinonoid stretching of PMO can be observed at 1540 and 1603 cm^{-1} respectively. The C-N stretching is confirmed through a peak at 1382 cm^{-1} [32]. The aromatic C-H out of plane bending vibration appears at 826 cm^{-1}. The SO_2 stretching appears around 1160 cm^{-1}. The dopant chloride ion appears at 565 cm^{-1}. The aromatic C-H stretchings are observed at 2873 and 2957 cm^{-1}. The aliphatic C-H symmetric and antisymmetric stretchings appear at 3041 and 3104 cm^{-1} respectively. During the polymerization of MO, the Fe^{3+} is converted into Fe^0. The iron nano particle appears at 609 cm^{-1}. A small hump at 1617 cm^{-1} confirms the presence of O-H bending vibration of SO_3H group of MO. It is very important to note that during the

polymerization of MO under strongly acidic condition the SO_3Na group of MO is converted into $-SO_3H$ group to some extent. The presence of $-SO_3H$ group improves the solubility of water.

Fig. 1b confirms the FTIR spectrum of PCL-PMO diblock copolymer initiated by PMO as a macromolecular initiator. The $-SO_3H$ group of MO was involved in the ROP of CL. The important peaks of PCL are described below. The O-H stretching of hydroxyl end capped PCL is noted at 3446 cm^{-1}. The C-H symmetric and antisymmetric stretching of PCL is referred at 2859 and 2943 cm^{-1} respectively. The aliphatic carbonyl stretching of PCL can be seen at 1716 cm^{-1}. The recent literature explained the slight shifting of carbonyl stretching due to the nature of the initiator [19-21]. The aliphatic C-O-C ester linkage of PCL appears at 1043 cm^{-1}. The C-H out of plane bending vibration of PCL appears at 718 cm^{-1}. The FTIR spectrum of PMO-PCL-PTHF triblock copolymer is shown in Fig. 1c. The tetrahydrofuronium ion is seen at 1549 cm^{-1} [28]. The remaining peaks are similar to that of PCL. Thus, the appearance of tetrahydrofuronium ion confirms the structure of triblock copolymer.

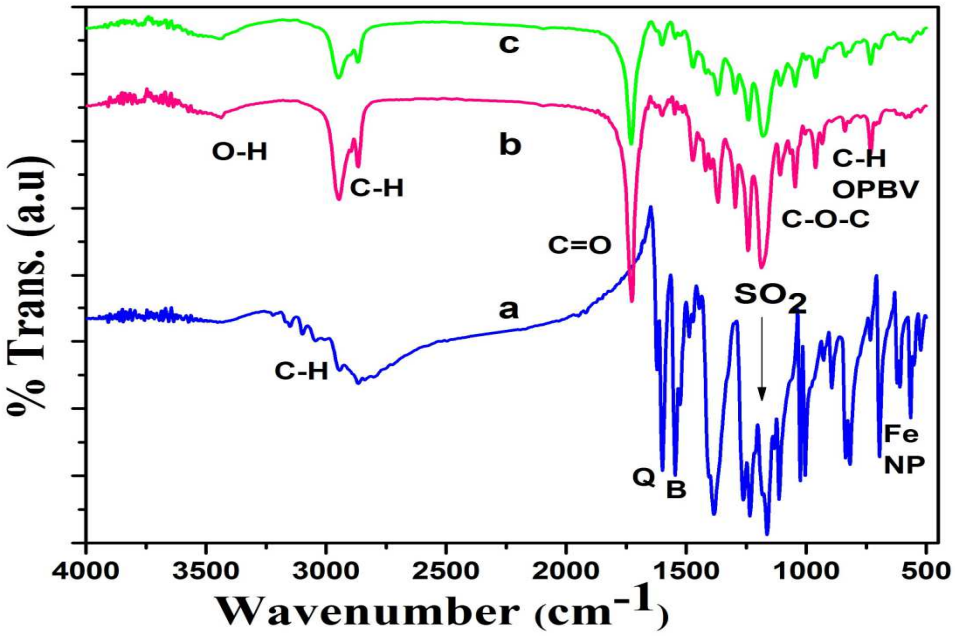

Figure 1. FTIR spectrum of (a) PMO, (b) PMO-b-PCL, (c) PMO-b-PCL-b-PTHF

UV- vis spectroscopy

The UV-visible spectrum of PMO and its di and triblock copolymer are given in Fig. 2. The UV-visible spectrum of PMO is given in Fig. 2a with the λ_{max} value of 375 nm. This is corresponding to the monomeric form of PMO [13-15]. Probably the dimeric form of MO might be oligomerized or polymerized. Fig. 2b indicates the UV-visible spectrum of PMO-PCL diblock copolymer with the λ_{max} value of 335 nm. The ROP of PCL in the presence of PMO was blue shifted the absorbance spectrum. This can be explained in terms of chain extension process. The added PCL units with the PMO backbone through the sulphonic acid group simply quenched the absorbance spectrum. The important point noted here is the interruption in the plasamon resonance effect. Moreover, the interface region between the hydrophilic PMO and hydrophobic PCL reduced the polymer size to the nanometer level. The UV-visible spectrum of PMO-PCL-PTHF is represented in Fig. 2c. Here the λ_{max} value was blue shifted to 323 nm. The decrease in wavelength might be associated with the reduction in polymer size and which can further be supported by FESEM result.

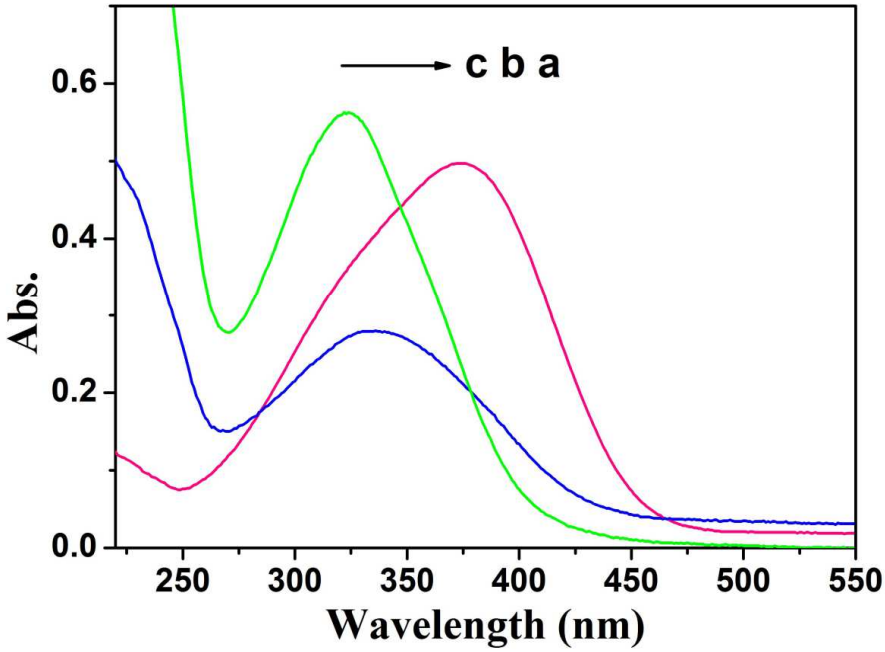

Figure 2. UV-visible spectrums of (a) PMO, (b) PMO-b-PCL, (c) PMO-b-PCL-b-PTHF

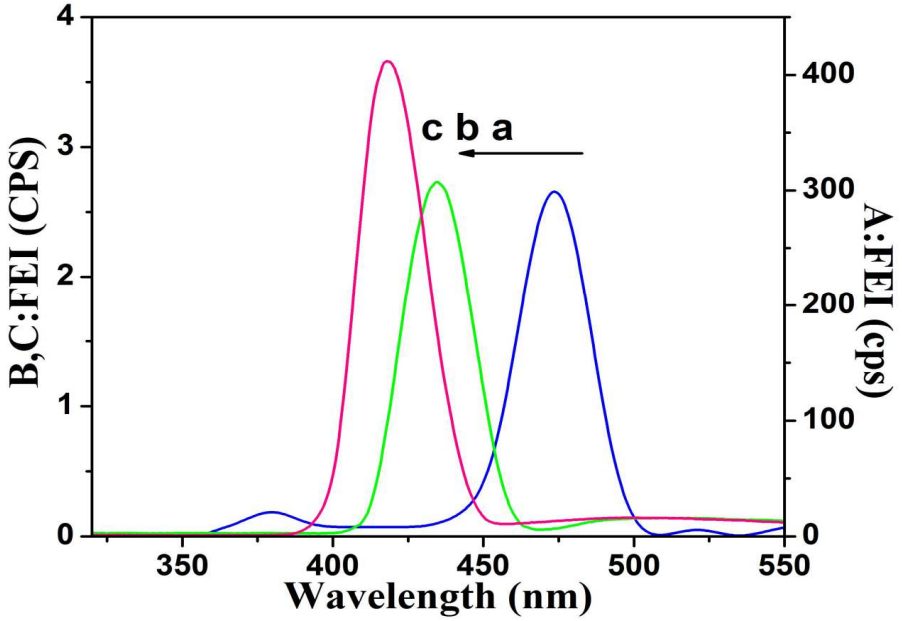

Figure 3. Fluorescence emission spectrum of (a) PMO, (b) PMO-b-PCL, (c) PMO-b-PCL-b-PTHF

Fluorescence study

The peculiar property of PMO dye is fluorescence. A strong fluorescence emission peak of PMO appears at 473 nm with FEI value of 304 cps (Fig. 3a). After the structural modification of PMO with PCL via insitu polymerization method, the PCL acts as a quencher. It means that the PCL chains are attached to the SO_3H group of PMO. Hence the fluorescence emission peak was blue shifted to 435 nm with the FEI of 2.80 cps (Fig. 3b). The quenching effect offered by PCL towards Eosin Y dye was studied by our research team [19]. In the present investigation, the quenching effect can be explained as follows: (i)The reduction in peak intensity is associated with the low

concentration of PMO. During the ROP of CL, the monomer to initiator ratio was maintained at 100. (ii)The SO_3H group of PMO was chemically attached to the PCL chains. Such a hydrophobic modification of hydrophilic polymer leads to the formation of nano micelles in the interface region. This can be further discussed in the FESEM study. The chemical modification of PMO by PCL suddenly dropped the FEI value. Due to the chemical modification, nano particle formation had occurred in the interface region and the FEI was reduced with blue shifting. The FEI of PMO-PCL-PTHF triblock copolymer is exhibited in Fig. 3c with the FEI of 3.6 cps at 418 nm. After the triblock copolymer formation the FEI was reduced. When compared to the PMO-PCL diblock copolymer the present system, PMO-PCL-PTHF exhibits a little bit higher FEI value. This can be explained as follows. (i)Introduction of a hydrophilic ether linkage ended with tetrahydrofuronium cation increased the charge carriers. (ii)The introduction of hydrophilic PTHF into the hydrophobic PCL again leads to the formation of nano particle with size reduction. (iii)The existence of charge mobility on the triblock copolymer backbone.

DSC study

The phase transition in the polymeric materials can be identified through the DSC measurement. The DSC thermogram of HCl doped PMO (Fig. 4a), diblock copolymer (Fig. 4b) and triblock copolymer (Fig. 4c) were analyzed through the DSC measurements as mentioned in Fig. 4. The homo PMO did not exhibit any T_g or T_m in the given range of temperature. This confirms the amorphous nature of PMO. The diblock copolymer exhibits a melting peak at 62.1^oC. This corresponds to the T_m of PCL. The triblock copolymer shows one sharp melting peak at 60.3^oC [19-21]. The reduction in melting temperature by 2^oC is depicted to the hydrophilic segments of PTHF. The hydrophilic PTHF can readily adsorb the moisture from the environment and hence reduce the T_m. After the triblock copolymer formation the molecular weight was increased. Even then the T_m value was suppressed due to the moisture absorbance of PTHF moieties.

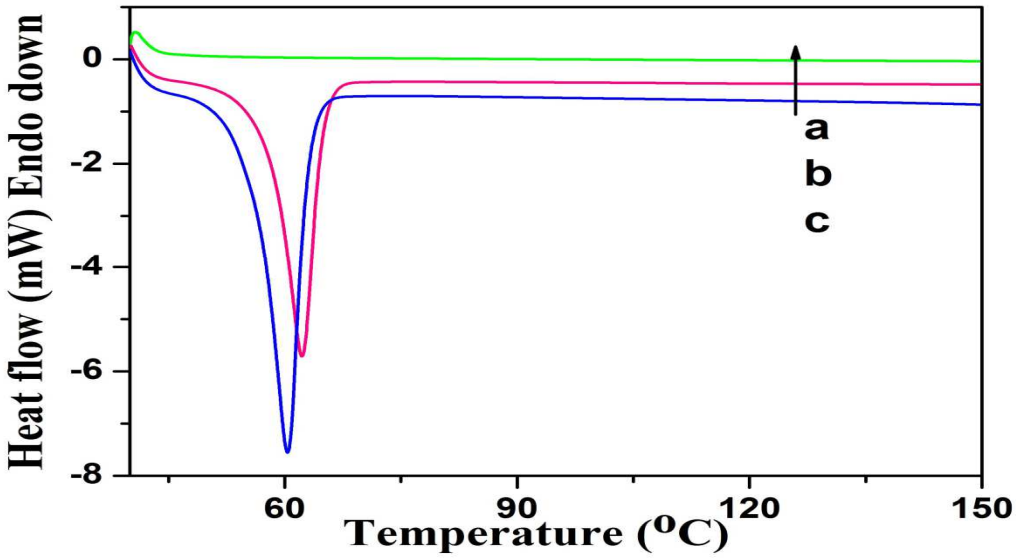

Figure 4. DSC thermogram of (a) PMO, (b) PMO-b-PCL, (c) PMO-b-PCL-b-PTHF

TGA study

The thermal stability of polymers under air atmosphere was studied by TGA. Fig. 5a represents the TGA thermogram of the homopolymer, PMO with two step degradation process. The first minor weight loss around 320^oC is explained by the removal of SO_2 gas from MO unit. The further increase in temperature led to the degradation of PMO backbone. The PMO backbone degradation was considered a major weight loss in PMO. After the degradation, above 650^oC the system exhibits approximately 43% weight residue remained. This is due to the presence of aromatic carbonaceous matters. Heating the PMO in the presence of atmospheric air leads to the oxidation reaction and forms the more rigid quinonoid structure. It means that the benzenoid ring is oxidized to more rigid quinonoid ring. Fig. 5b indicates the TGA thermogram of PMO-PCL diblock copolymer. Here also one can observe a two step degradation process. The first minor weight loss before 250^oC is associated with the removal of moisture and the degradation of PCL-PMO linkage with the liberation of SO_2 gas. Around 265^oC the PCL backbone undergoes to degradation reaction. Our earlier publication showed the degradation of PCL around 400^0C [21]. In the present investigation, the T_d of PCL was totally depressed due to the amorphous and hydrophilic nature PMO dye. Above 650^oC it shows 41% weight residue remained. Fig. 5c reveals the TGA thermogram of PMO-PCL-PTHF triblock copolymer. The thermogram exhibits a three step degradation process. The first minor weight loss

below 200°C is ascribed to the removal of PMO segments from the triblock copolymer. The major second weight loss step is noted around 390°C corresponding to the degradation of PCL backbone [21]. The third minor weight loss around 475°C is depicted to the degradation of PTHF segments. Even though, the PTHF is a hydrophilic one, which can offer more hydrogen bonding through its ether linkages. As a result the thermal degradation of PCL backbone was shifted to higher temperature. Above 650°C it exhibits 34% weight residue remained. In overall comparison, the PMO homopolymer exhibited a higher thermal stability.

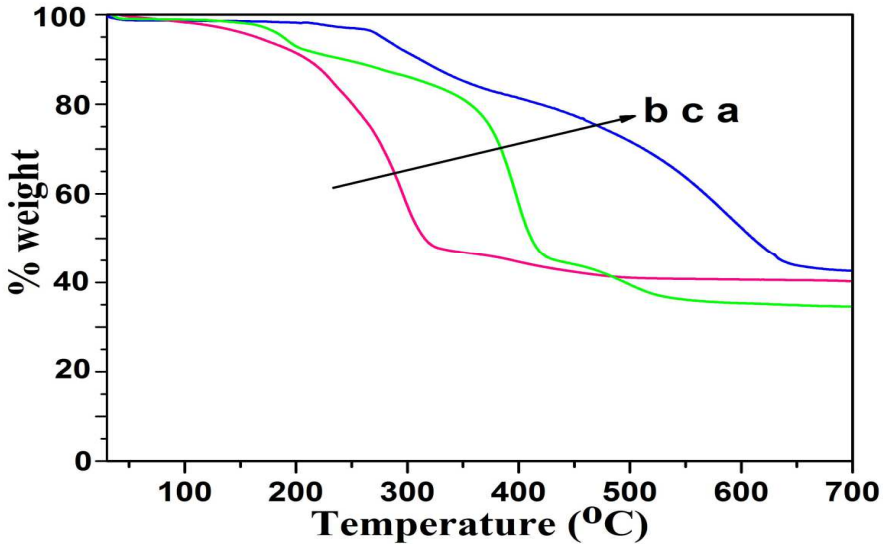

Figure 5. TGA thermogram of (a) PMO, (b) PMO-b-PCL, (c) PMO-b-PCL-b-PTHF

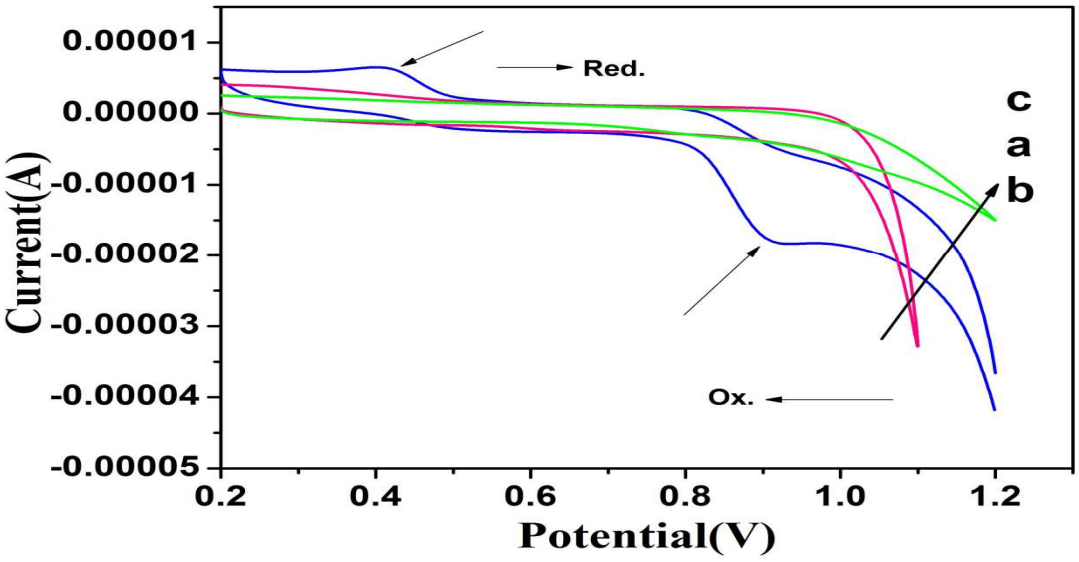

Figure 6 Cyclic voltammetry of (a) PMO, (b) PMO-b-PCL, (c) PMO-b-PCL-b-PTHF

Cyclic voltammetry study

The redox potential of electroactive dye molecule can be studied by CV measurements. The CV experiment was carried out in 1M HCl medium. PMO exhibits two oxidation and two reduction peaks. The first oxidation peak occurred at 0.91V with the reduction potential of 0.86V. The second oxidation and reduction peaks appeared at 0.40 and 0.41V respectively. The primary oxidation reaction took place at 0.9 V with the removal of one of the lone pair of electrons from the N-$(CH_3)_2$ group. The secondary oxidation at 0.40V led to the removal of further one of the lone pair of electrons. The primary and the secondary oxidation led to the formation of nitrogen radical and nitrogen

diradical. The primary oxidation is somewhat more difficult than the secondary oxidation reaction. The low oxidation potential of nitrogen can be explained on the basis of steric effect caused by two bulky methyl substituents present on the nitrogen atom of PMO. After the diblock (Fig. 6b) and triblock (Fig. 6c) copolymer formation the redox peaks disappeared. This is due to the low concentration of oxidizable PMO. This proves the poor electroactivity nature of both diblock and triblock copolymer.

GPC study

Polymerization of MO in the presence of $FeCl_3$ was confirmed by GPC measurement (Fig. 7a). The chromatogram shows the weight average molecular weight (M_w) and number average molecular weight (M_n) of PMO as 2395 g/mol and 939 respectively. The polydispersity (P.D) was determined as 2.6 which confirmed the occurrence of crosslinking or branching. The GPC analysis confirms the polymer formation from its monomer via determining the both number average and weight average molecular weights. Fig. 7b shows the GPC of PMO-PCL diblock copolymer. The system exhibits both M_n and M_w of 1726 and 4017 g/mol respectively. The P.D value was calculated as 2.3. Both M_n and M_w were found to be very low when compared to our earlier publication [21]. This is because the initiating efficiency depends on the nature and available functional groups and miscibility of the initiating species. Fig. 7c confirms the GPC of PMO-PCL-PTHF system. The M_n and M_w were calculated as 1644 and 5357 g/mol respectively. The P.D value was determined as 3.2. The high P.D value confirmed that the resultant polymer does not have narrow molecular weight. It means the O-H end of PCL can initiate the ROP of THF with various degree of polymerization. The variation in the degree of polymerization motivated to the crosslink or branched polymer formation.

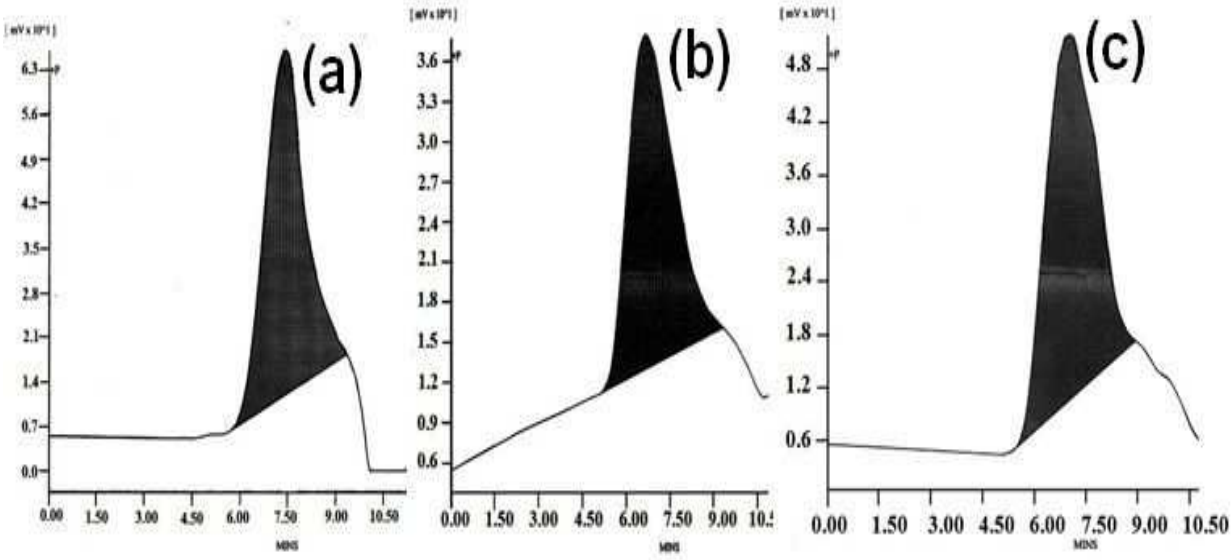

Figure 7. GPC traces of (a) PMO, (b) PMO-b-PCL, (c) PMO-b-PCL-b-PTHF

FESEM study

The surface morphology of $FeCl_3$ initiated chemical polymerization of MO is shown in Fig. 8a.The image exhibits the presence of nano particles with and without agglomerated structure. The average size of non-agglomerated iron particle was determined as 48nm. The appearance of iron nano particle is due to the reduction of Fe^{3+} into Fe^0. Fig. 8b shows the FESEM image of PMO-PCL diblock copolymer. The broken stone like morphology with some voids confirms the surface morphology of PCL [19-21]. In this case, the iron nano particles were dispersed on the PMO-PCL backbone. The presence of micro voids added more value to the diblock copolymer material as a biomaterial particularly used in the drug delivery application. Fig. 8c confirms the surface morphology of PMO-PCL-PTHF triblock copolymer. Here one can see the broken stone like morphology, micro voids and some agglomerated iron nano particles. The presence of PTHF segments did not alter the surface morphology.

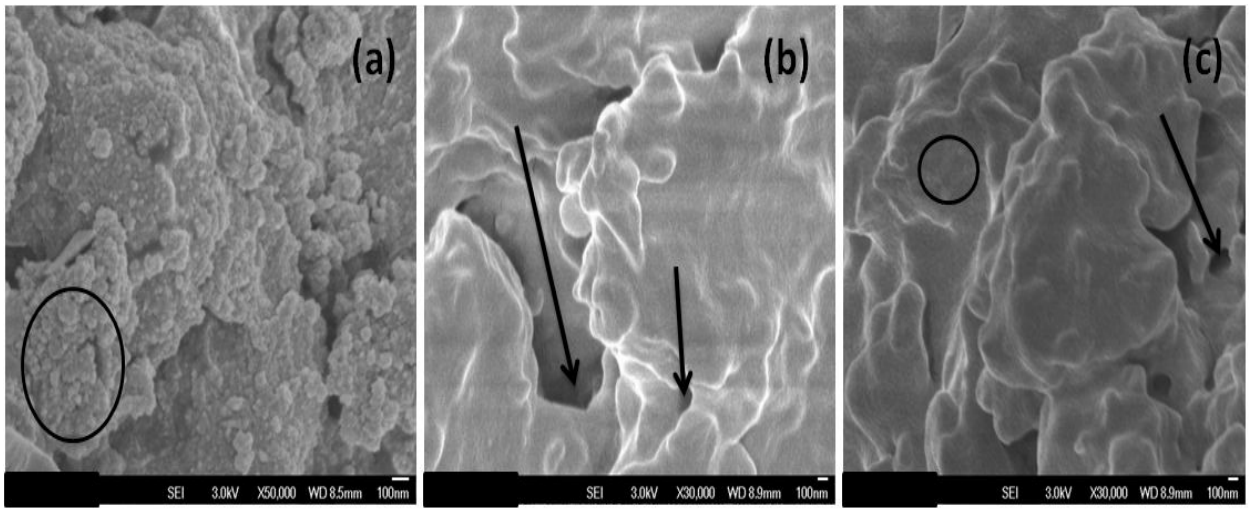

Figure 8. FESEM images of (a) PMO, (b) PMO-b-PCL, (c) PMO-b-PCL-b-PTHF

Conductivity study

The effect of temperature on the conductivity of polymers was studied and shown in Fig. 9. The homo PMO (Fig. 9a) exhibited higher electrical conductivity while varying the temperature from 290K to 304K. While increasing the temperature the conductivity was also linearly increased. While increasing the temperature the resonance stabilization was increased due to the high activation energy. Fig. 9b represents the plot of Temperature Vs Conductivity for PMO-PCL diblock copolymer system. The interesting point noted here is while increasing the temperature the conductivity was smoothly increased initially thereafter a steep increase of conductivity. Below the T_g of PCL the electron mobility in PMO was restricted. But above the T_g, the electron mobility was freely available due to the segmental mobility of polymers. The segmental mobility could increase the conductivity beyond certain level due the restriction in chain mobility imposed by the chemically conjugated PCL chains with PMO. Moreover, PCL is a soft insulator with low T_g [21]. Fig. 9c demonstrates the effect of temperature on the electrical conductivity of PMO-PCL-PTHF triblock copolymer system. Here also one can note that the increase in electrical conductivity during the increase in temperature. Above 300K the temperature was steeply increased due to the segmental mobility of PCL and PTHF. In the case of PTHF the polymer chains were ended with tetrahydrofuronium cation. The increase in number of positive charges led to the increase in electrical conductivity through the hole-hole mechanism. The present investigation proves that the conductivity of a polymer could be improved through hole-hole mechanism above the T_g of that polymer. It means both electron mobility and positively charged species mobility increased the conductivity of a material. The hopping mechanism applied here is similar to that of poly(phthalocyanine) system [33].

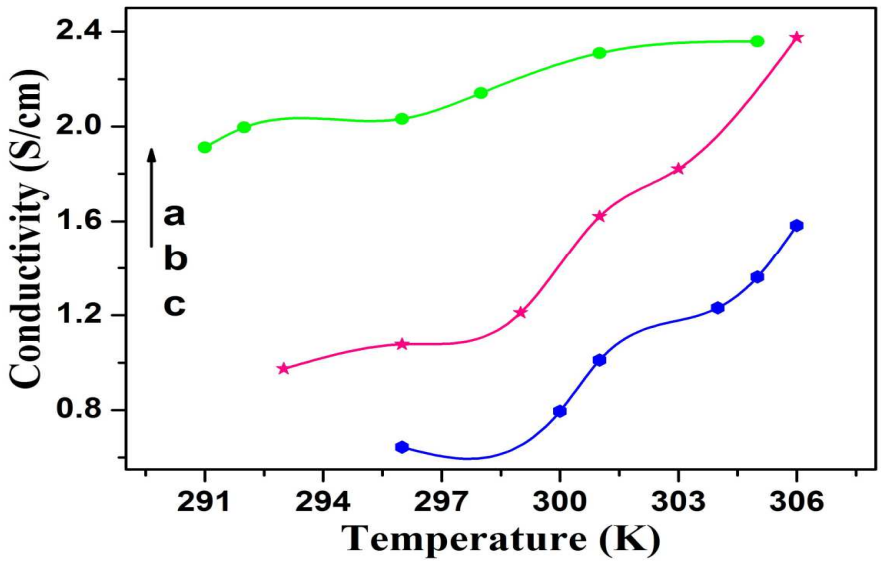

Figure 9 Plot of Temperature Vs. conductivity of (a) PMO, (b) PMO-b-PCL, (c) PMO-b-PCL-b-PTHF

Humidity sensor study

Since the PMO is an electrically conducting polymer the application of such a polymer is extended to the humidity sensor field. The plot of %RH against Resistivity is shown in Fig. 10. Fig. 10a represents the fact that while increasing the relative humidity the electrical conductivity was increased. On the other hand, one can express that while increasing the % RH the resistivity of PMO was found to be reduced. This confirms that PMO is a typical electrically conducting polymer. Fig. 10b-c demonstrates the plot of % RH Vs Resistivity for PMO-PCL and PMO-PCL-PTHF copolymers. These two systems are also followed in the above said trend for PMO system. Among the three systems, homo PMO, PMO-PCL diblock copolymer, PMO-PCL-PTHF triblock copolymer, the former one exhibits good result [34]. The latter two cases exhibit lower value due to the structural modification process. The structural modification process imports the steric effect and destabilization of resonance effect. At the same time the structural modification improved the environmental stability.

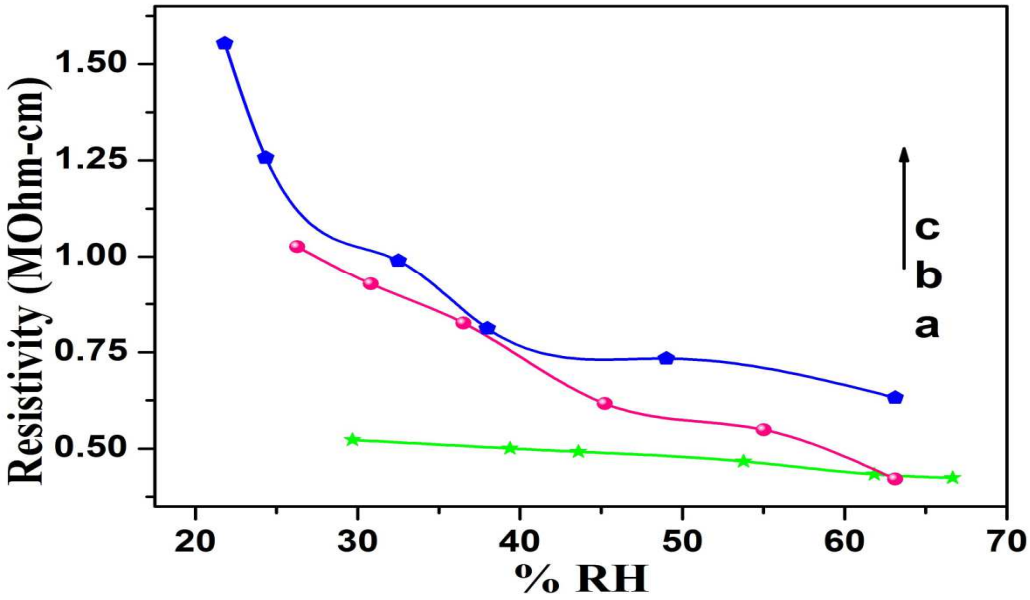

Figure 10. Plot of %RH Vs. Resistivity of (a) PMO, (b) PMO-b-PCL, (c) PMO-b-PCL-b-PTHF

CONCLUSION

The important points of the present investigation is summarized here as conclusion. The appearance of C=O stretching at 1716 cm^{-1} confirms the block copolymer formation with CL. The blue shift in the absorbance spectrum of block copolymer confirms the reduction in size of the polymer. The emission peak of the block copolymer confirms the presence of PMO moieties in the backbone. The increase in molecular weight of block copolymer confirms the ROP of CL and THF in the presence of SO as a catalyst. The PMO exhibited the highest thermal stability. FESEM confirms the formation of polymer nano particles in the interface region of block copolymer. The primary oxidation potential of PMO is higher than that of the secondary oxidation. The PMO exhibited the highest thermal conductivity and humidity sensing property than the block copolymers. The present investigation concludes that the process ability of conducting polymer can be increased by the way of making copolymer with conventional monomers.

Acknowledgements

The authors gratefully acknowledge Mrs. G. Vijayalakshmi, Assistant Professor of English for her valuable help during this manuscript preparation work.

REFERENCES

[1] L. Tan, Q. Xie, S. Yao. *Electroanal.* **2004** 16 1592-1597.
[2] H. Yao, Y. Sun, X. Lin, Y. Teng, L. Huang. *Electrochim. Acta.* **2007, 52,** 6165-6171.
[3] C. Fang, X. Tang, X. Zhou, Anal. Sci. **1999** (15) 41-46.
[4] Q. Xu, L.L. Chen, G.J. Lu, X.Y. Hu, H.B. Li, L.L. Ding, Y. Wang. *J. Appl. Electrochem*. 41, 2011**,** 143-149.
[5] R. Mazaikiene, K. Balskus, O.E. Lorka, G. Niawsa, R. Meskys, A. Malinaykum.*Vis. Spect.* **2009,** 51, 238-247.

[6] R. Pauliukaite, C.M.A. Brett.*Electroanal*. **2008,** 20, 1275-1285.
[7] X. Lin, Q. Zhuang, J. Chen, S. Zhang, Y. Zheng. *Sensors Actuators B.*, **2007,** 125, 240-245.
[8] Q. Wan, X. Wang, N. Yasg.*Polymer*. **2006,** 47, 7684-7692.
[9] D.G. Dilgin, D. Glisor, H.I. Gokcel, Z.D. Dursun, Y. Dilgin.*Microchim. Acta.*, **2011,** 173(3-4) 469-476.
[10] R. Pauliukaite, A. Selskiene, A. Malinaybg, C.M.A. Brett.*Thin Solid Films*, **2009,** 517, 5435-5441.
[11] X. Liu, B. Li, M. Ma, G. Zhan, C. Liu, C. Li.*Microchim. Acta.* **2012,** 176, 123-129.
[12] S.M. Chen, G.H. Chiang.*J. Appl. Electrochem*. **2005,** 575, 125-137.
[13] S. Ghosh, L.K. Dey.*Supramol. Chem.*, **2009,** 21, 591-596.
[14] T. Sato, K. Nakagawa, H. Fujiwan. *Optical Rev.* **2002,** 9, 154-158.
[15] K. Murakami, T. Saro, N. Kure, K.Ishii, T. Yasunaga. *Biopolym.*. **2004,** 22, 2035-2044.
[16] L.J. Liu, S.J. Cai, Y. Tan, J.J. Du, H.L. Dong, L. Q. Liao.*J. Polym. Sci. Part A: Polym.Chem.*. **2009,** 47, 6214-6222.
[17] Z. Zhong, M.J.K. Ankone, P.J. Dijksfra, C.Birg, J. Feijen, .*Polym. Bull.* **2007,** 46, 51-57.
[18] I.H. Lin, C.C. Cheng, Y.C. Yen, F.C. Chong. *Macromolecules* **2010,** 43, 1245-1252.
[19] H.H. Chen, R. Anbarasan, L.S. Quo, P.H. Chen. *J. Mater. Sci.* **2011,** 46, 1796-1805.
[20] H.H. Chen, R. Anbarasan, L.S. Quo, P.H. Chen. *Mater. Chem. Phys.* **2011,** 126, 584-590.
[21] B. Meenarathi, H.H. Chen, P.H. Chen, R.Anbarasan. *J. Polym. Res.* **2013,** 20, 118-130.
[22] M. Sobczak, W. Kolodziejski.*Molecules*, **2009,** 14,621-632.
[23] S.S. Liow, L.K. Nidjaja, V.T. Lippk, M. Abad.*Exp. Polym. Lett.* **2009,** 3,159-167.
[24] I. Kerman, L. Toppare, F. Yilmaz, Y. Yogci. *J. Macromol. Sci. Part A: Pure Appl. Chem.*.**2005,** 42, 509-520.
[25] B.C. Wilson, C.W. Jones, *Macromolecules*, **2004,** 37, 9709-9714.
[26] A. Aourishi, S.S.A. Deyab, H.H. Shakri, Chin. *J. Polym. Sci.* **2010,** 28, 305-310.
[27] A. Aourishi, S.S.A. Deyab, H.A. Shakri, *Molecules* **2010,** 15, 1398-1407.
[28] P. Shokrollahi, *Iran. Polym. J.* **2010,** 19, 65-74.
[29] M.I. Ferrahi, M. Belbachir, *Int. J. Mol. Sci*. **2003,** 4 (6), 312-325.
[30] O. Akbulnt, I. Tasighchi, S. Kubor, Y.S. Horn, A.M. Mayer, *Electrochim. Acta.* **2007,** 52, 1983-1989.
[31] R. Anbarasan, T. Vasudevan, A. Gopalan, *Polym. News*, **1999,** 24, 391-395.
[32] S. Radhika, K. Duraimurugan, I. baskaran, R. Anbarasan, *J. Mater. Sci.* **2009,** 44, 3542-3555**.**
[33] S. Saravanan, C.J. Mathai, M.R. Anantharaman, P.V. Prabhakaran, ,*J. Appl. Polym. Sci.* **2004,** 91, 2529-2535.
[34] A.V. Kulkarni, A.K. Viswanath, R.C. Aiyer, P.K. Khanna, *J. Polym. Sci. Part B Polym. Phys.* **2005,** 43,161-2168.
[35] S. Dash,P.N. Murthy, L. Nath, P. Choudhury. *Acta Polonica Pharmacuetica.*, **2010,** 67, 217-223.